IL NUOVO CIMENTO Vol. 35 C, N. 2 Marzo-Aprile 2012
DOI 10.1393/ncc/i2012-11198-4

Colloquia: Transversity 2011

Extraction of TMDs with global fits

S. Melis(1), M. Anselmino(2)(3), V. Barone(4)(5), M. Boglione(2)(3),
U. D'Alesio(6)(7), F. Murgia(7) and A. Prokudin(8)

(1) *ECT*, Villa Tambosi - Strada delle Tabarelle 286, Villazzano, Trento, Italy*
(2) *Dipartimento di Fisica Teorica, Università di Torino - Via Pietro Giuria 1, Torino, Italy*
(3) *INFN, Sezione di Torino - Via Pietro Giuria 1, Torino, Italy*
(4) *Di.S.T.A., Università del Piemonte Orientale "A. Avogadro" - Alessandria, Italy*
(5) *INFN, Gruppo Collegato di Alessandria - Alessandria, Italy*
(6) *Dipartimento di Fisica, Università di Cagliari, Cittadella Universitaria C.P. 170, Monserrato (CA), Italy*
(7) *INFN, Sezione di Cagliari - C.P. 170, Monserrato (CA), Italy*
(8) *Jefferson Laboratory - 12000 Jefferson Avenue, Newport News, VA, USA*

ricevuto il 2 Novembre 2011; approvato il 21 Dicembre 2011
pubblicato online il 23 Marzo 2012

Summary. — We present a brief review of our recent extractions of the Transverse-Momentum–Dependent distribution and fragmentation functions performed by analysing Semi-Inclusive Deep Inelastic Scattering and $e^+e^- \to h_1h_2 + X$ data on azimuthal asymmetries.

PACS 13.88.+e – Polarization in interactions and scattering.
PACS 13.60.-r – Photon and charged-lepton interactions with hadrons.
PACS 13.60.Le – Meson production.
PACS 13.85.Ni – Inclusive production with identified hadrons.

1. – Introduction

Collinear parton distribution functions (PDFs) depend on the fraction x of hadron momentum carried by the parton and on the virtuality of the hard probe, Q^2. Transverse-Momentum–Dependent parton distributions (TMDs) additionally depend on the intrinsic transverse momentum of the parton, $\boldsymbol{k}_\perp$, thus describing the nucleon structure, in the full three-dimensional partonic momentum space.

At leading twist, nucleons can be described by 8 TMDs [1-3]. Each TMD represents a particular physical aspect of spin-orbit correlations at partonic level. Semi-Inclusive Deep Inelastic Scattering (SIDIS) and Drell-Yan (DY) are the key processes where the three-dimensional structure of the nucleon can be studied. Both these processes depend on two scales: the virtuality of the hard probe, Q^2, which is assumed to be large, and the transverse momentum $P_T \simeq \Lambda_{QCD} \ll Q$ of the final detected hadron (in SIDIS) or of the dilepton pair (in DY). Large Q^2 values ensure the applicability of the QCD parton model while the second (small) scale, P_T, can be related to the transverse motion of partons. In this kinematical regime (TMD) factorization applies, thus allowing the study of TMDs.

Drell-Yan processes are the cleanest processes where TMDs can be observed due to the pure leptonic final state. However they are experimentally difficult to realize due to their very small cross section. Moreover, polarized DY experiments have never been performed. On the contrary, SIDIS processes, despite their hadronic final state, have provided a large amount of data from which many TMDs could be extracted. Here we present a brief review of our recent results on the phenomenological study of the TMDs, mainly from SIDIS data.

2. – The Sivers function

In ref. [4] we presented an extraction of the Sivers distribution functions based on a fit of SIDIS experimental data from the HERMES [5] and COMPASS [6,7] Collaborations. Data from HERMES [5] presented an unexpectedly large $A_{UT}^{\sin(\phi_h-\phi_S)}$ asymmetry for K^+ production, about twice the analogous asymmetry for π^+. Such a large asymmetry suggested an important role of the sea Sivers functions. Our analysis confirmed this expectation finding a large contribution of the $\bar{s}$-Sivers function.

A new HERMES data analysis [8], based on a much larger statistics, while confirming the previous pion data, shows a smaller asymmetry for K^+ production. These new data prompted us to perform a new analysis. Here we present a preliminary phenomenological fit of HERMES proton and COMPASS deuteron data. The Sivers functions have been parametrized as

$$\Delta^N f_{q/p^\uparrow}(x,k_\perp) = -\frac{2k_\perp}{M_N} f_{1T}^\perp(x,k_\perp) = 2\,\mathcal{N}_q(x)\,h(k_\perp)\,f_{q/p}(x,k_\perp), \tag{1}$$
$$\mathcal{N}_q(x) = N_q\,x^{\alpha_q}(1-x)^{\beta_q}\,\frac{(\alpha_q+\beta_q)^{(\alpha_q+\beta_q)}}{\alpha_q^{\alpha_q}\beta_q^{\beta_q}}\,, \quad h(k_\perp) = \sqrt{2e}\,\frac{k_\perp}{M_1}\,e^{-k_\perp^2/M_1^2},$$

where $N_q \in [-1,1]$, α_q, β_q and M_1 (GeV/c) are free parameters. M_N is the nucleon mass and $f_{1T}^\perp(x,k_\perp)$ is the Sivers function in the Amsterdam notation [9]. For the unpolarized PDFs and FFs, we adopt a factorized Gaussian form

$$f_{q/p}(x,k_\perp) = f_q(x)\,\frac{1}{\pi\langle k_\perp^2\rangle}\,e^{-k_\perp^2/\langle k_\perp^2\rangle}, \qquad D_q^h(z,p_\perp) = D_q^h(z)\,\frac{1}{\pi\langle p_\perp^2\rangle}\,e^{-p_\perp^2/\langle p_\perp^2\rangle}, \tag{2}$$

with $\langle k_\perp^2\rangle = 0.25\,(\mathrm{GeV}/c)^2$ and $\langle p_\perp^2\rangle = 0.20\,(\mathrm{GeV}/c)^2$ as found in ref. [10]. Collinear PDFs are taken at Leading Order (LO) as in ref. [11] while for the FFs we used the DSS set [12].

We fitted HERMES proton and COMPASS deuteron data from refs. [6,8] (209 points) including only Sivers functions for u and d quarks, corresponding to seven free parameters, shown in table I. The results we obtain are rather satisfactory, with a χ^2_{dof} of about 1.06. Such results are similar to those obtained in ref. [13]. The Sivers functions are plotted in the right panel of fig. 1.

TABLE I. – χ^2 *and best values of the parameters.*

	$\chi^2_{dof} = 1.06$	
$N_u = 0.40$	$\alpha_u = 0.35$	$\beta_u = 2.6$
$N_d = -0.97$	$\alpha_d = 0.44$	$\beta_d = 0.90$
	$M_1^2 = 0.19\,\text{GeV}^2$	

As shown in the left panel of fig. 1, the new HERMES data on kaon production can be described reasonably well without any sea Sivers function contribution, although their inclusion in the fit procedure can slightly improve the χ^2_{dof} [14]. The gray band in fig. 1 represents the statistical error of the fitting procedure, calculated as in ref. [4].

3. – Transversity and Collins functions from SIDIS and e^+e^- data

The transversity function is one of the fundamental PDFs appearing in collinear approximation. However, due to its chiral-odd nature, it cannot be observed in deep inelastic processes. The double transversely polarized DY is the golden channel for its observation but, as noticed in the introduction, there are no data available for polarized DY processes. Transversity can be studied in SIDIS processes where it appears convoluted with the chiral-odd Collins fragmentation function [15]. The Collins fragmentation function can be probed in $e^+e^- \to h_1h_2X$ processes. Therefore a combined fit of SIDIS asymmetries $A_{UT}^{\sin(\phi_h+\phi_S)}$ together with $e^+e^- \to h_1h_2X$ data allows the simultaneous extraction of the transversity distribution and the Collins fragmentation functions.

In ref. [16] we analysed the data released by the HERMES [5] and COMPASS [6] Collaborations for SIDIS, and the A_{12}^{UL} data by the Belle Collaboration [17] for the $e^+e^- \to \pi_1\pi_2X$ process. The transversity and the Collins functions are parametrized in

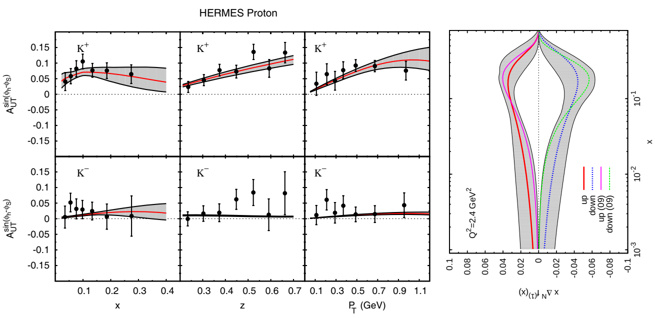

Fig. 1. – The fit of HERMES data [8] for kaon production is presented in the left panel. The right panel shows the first moment of the Sivers functions extracted from the fitting procedure presented in this paper and those obtained in ref. [4].

TABLE II. – *Best values of the free parameters for the u and d transversity distribution functions and for the favoured and unfavoured Collins fragmentation functions* [16].

$N_u^T = 0.64 \pm 0.34$	$N_d^T = -1.00 \pm 0.02$	$N_{fav}^C = 0.44 \pm 0.07$	$N_{unf}^C = -1.00 \pm 0.06$
$\alpha = 0.73 \pm 0.51$	$\beta = 0.84 \pm 2.30$	$\gamma = 0.96 \pm 0.08$	$\delta = 0.01 \pm 0.05$
		$M_h'^2 = 0.91 \pm 0.52\,\mathrm{GeV}^2$	

a simple factorized form [16]:

$$\Delta_T q(x, k_\perp) = \frac{1}{2}\mathcal{N}_q^T(x)\,[f_{q/p}(x) + \Delta q(x)]\frac{e^{-k_\perp^2/\langle k_\perp^2\rangle}}{\pi\langle k_\perp^2\rangle}, \tag{3}$$

$$\mathcal{N}_q^T(x) = N_q^T\, x^\alpha (1-x)^\beta\, \frac{(\alpha+\beta)^{(\alpha+\beta)}}{\alpha^\alpha \beta^\beta},$$

$$\Delta^N D_{h/q^\uparrow}(z, p_\perp) = \frac{p_\perp}{zM_h} H_1^\perp(z, p_\perp) = 2\mathcal{N}_q^C(z)\, D_{h/q}(z) h(p_\perp)\, \frac{e^{-p_\perp^2/\langle p_\perp^2\rangle}}{\pi\langle p_\perp^2\rangle}, \tag{4}$$

$$\mathcal{N}_q^C(z) = N_q^C\, z^\gamma (1-z)^\delta\, \frac{(\gamma+\delta)^{(\gamma+\delta)}}{\gamma^\gamma \delta^\delta}, \qquad h(p_\perp) = \sqrt{2e}\,\frac{p_\perp}{M_h'}\, e^{-p_\perp^2/M_h'^2},$$

where $-1 \le N_q^T \le 1$, $-1 \le N_q^C \le 1$. In eq. (4) M_h' is the mass of the produced hadron while $H_1^\perp$ denotes the Collins function in the Amsterdam notation. $\Delta q(x)$ is the helicity distribution and it is taken from ref. [18].

We fitted data assuming only the existence of u and d transversity functions and separating the Collins functions in favored and unfavored fragmentation functions. This choice implies the use of 9 free parameters. We obtained a $\chi^2_{dof} = 1.3$ [16]. The best fit parameters can be found in table II.

4. – Boer-Mulders function from unpolarized SIDIS data

In ref. [19] we performed an analysis of the $\cos 2\phi$ asymmetry recently measured by the COMPASS [20, 21] and HERMES [22] Collaborations in unpolarized SIDIS. At leading-twist the only $k_\perp$-dependent term contributing to the $\cos 2\phi$ asymmetry contains the Boer-Mulders distribution $h_1^\perp$ coupled to the Collins fragmentation function $H_1^\perp$ of the produced hadron. This contribution to the cross section is given by [9]

$$\left.\frac{d^5\sigma_{\rm BM}^{(0)}}{dx\,dy\,dz\,d^2\boldsymbol{P}_T}\right|_{\cos 2\phi} = \frac{4\pi\alpha_{\rm em}^2 s}{Q^4}\sum_q e_q^2\, x(1-y)\int d^2\boldsymbol{k}_\perp \int d^2\boldsymbol{p}_\perp\, \delta^2(\boldsymbol{P}_T - z\boldsymbol{k}_\perp - \boldsymbol{p}_\perp) \times \frac{2\,\boldsymbol{h}\cdot\boldsymbol{k}_\perp\, \boldsymbol{h}\cdot\boldsymbol{p}_\perp - \boldsymbol{k}_\perp\cdot\boldsymbol{p}_\perp}{zM_N M_h}\, h_1^{\perp q}(x, k_\perp^2)\, H_1^{\perp q}(z, p_\perp^2)\cos 2\phi, \tag{5}$$

where $\boldsymbol{h} \equiv \boldsymbol{P}_T/P_T$. Other contributions to the $\cos 2\phi$ asymmetry come from twist-4 effects. Here we will consider only the twist-4 Cahn contribution. It has the form

$$\left.\frac{\mathrm{d}^5\sigma_{\mathrm{C}}^{(0)}}{\mathrm{d}x\,\mathrm{d}y\,\mathrm{d}z\,\mathrm{d}^2\boldsymbol{P}_T}\right|_{\cos 2\phi} = \frac{8\pi\alpha_{\mathrm{em}}^2 s}{Q^4}\sum_q e_q^2\, x(1-y)\int \mathrm{d}^2\boldsymbol{k}_\perp \int \mathrm{d}^2\boldsymbol{p}_\perp\, \delta^2(\boldsymbol{P}_T - z\boldsymbol{k}_\perp - \boldsymbol{p}_\perp) \times \frac{2\,(\boldsymbol{k}_\perp\cdot\boldsymbol{h})^2 - \boldsymbol{k}_\perp^2}{Q^2}\, f_1^q(x,k_\perp^2) D_1^q(z,p_\perp^2)\cos 2\phi. \tag{6}$$

Notice that the Cahn term is only a part of the complete, still unknown, twist-4 contribution.

The available data on $\langle\cos 2\phi\rangle$ do not allow a full extraction of the Boer-Mulders function. Thus we simply take $h_1^\perp$ to be proportional to the Sivers function $f_{1T}^\perp$,

$$h_1^{\perp q}(x,k_\perp^2) = \lambda_q\, f_{1T}^{\perp q}(x,k_\perp^2), \tag{7}$$

with a coefficient λ_q to be fitted to the data. The Sivers functions are taken from ref. [4], see also sect. **2**. Unpolarized PDFs and FFs are taken as in sect. **2** and the Collins functions as in sect. **3**. Fitting the HERMES and COMPASS data we found the following values for the coefficients λ_u and λ_d:

$$\lambda_u = 2.0, \qquad \lambda_d = -1.1. \tag{8}$$

This implies that $h_1^{\perp u}$ and $h_1^{\perp d}$ are both negative. The χ^2 per degree of freedom of our fit is $\chi^2_{dof} = 3.73$. This high value reflects our poor knowledge of the underlying Cahn mechanism, and of the possible dependence of $\langle k_\perp^2\rangle$ and $\langle p_\perp^2\rangle$ on x and z. More experimental information is needed to unravel this dependence. At present, the quality is good enough to draw some preliminary conclusion on the sign and the approximate size of the Boer-Mulders functions, which appear to be compatible with the theoretical expectations.

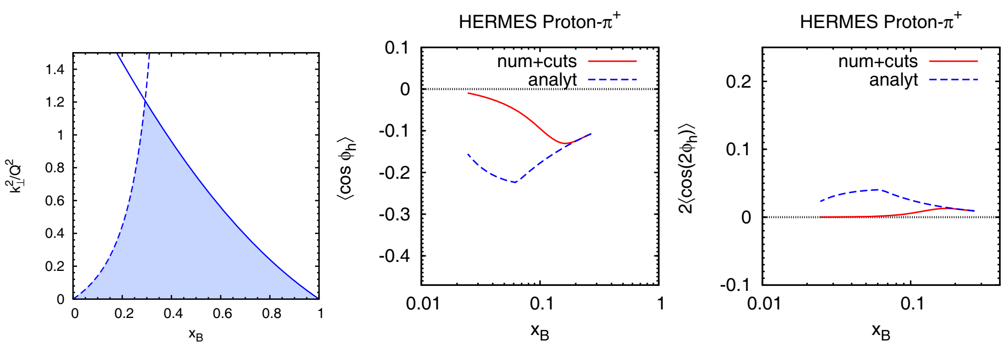

Fig. 2. – (Colour on-line) In the left panel the $k_\perp^2/Q^2$ phase space as determined by the bounds of eqs. (9) and (11). The allowed region, which fulfills both bounds, is represented by the shaded area below the solid line. The Cahn contribution to the $\langle\cos\phi_h\rangle$ and $\langle\cos 2\phi_h\rangle$ asymmetries is show in the central and right panels. The solid (red) line corresponds to the cahn contribution calculated with a numerical $k_\perp$ integration over the range $[0, k_\perp^{max}]$ given by eqs. (9) and (11). The dashed (blue) line is obtained by integrating over $k_\perp$ analytically.

5. – Partonic transverse motion in unpolarized SIDIS processes

In phenomenological analysis, the transverse momentum distribution of the TMDs is usually assumed to be a Gaussian. This is a convenient approximation as it allows to solve the $k_\perp$ integration analytically, integrating over the full $k_\perp$ range, $[0,\infty]$, and it leads to a successful description of many sets of data.

However, in some kinematical region the gaussian smearing is not sufficient to prevent large $k_\perp^2/Q^2$ contributions to the cross section. The large twist-4 Cahn effect found in ref. [19] is a remarkable example of such contributions.

A physical picture that allows us to put some further constraints on the partonic intrinsic motion is provided by the parton model, where kinematical limits on the transverse momentum size can be obtained by requiring the energy of the parton to be less than the energy of the parent hadron and by preventing the parton to move backward with respect to the parent hadron direction ($k_z < 0$). They give, respectively:

$$k_\perp^2 \le (2 - x_B)(1 - x_B)Q^2, \quad 0 < x_B < 1. \tag{9}$$

$$k_\perp^2 \le \frac{x_B(1 - x_B)}{(1 - 2x_B)^2}Q^2 \quad x_B < 0.5. \tag{10}$$

Notice that these are exact relations, which hold at all orders in $(k_\perp/Q)$.

The ratio $k_\perp^2/Q^2$, as constrained by eqs. (9) and (11), is shown in the left panel of fig. 2 as a function of x_B: from this plot it is immediately evident that, in the region spanned by present data from HERMES and COMPASS experiments ($x_b < 0.3$), eq. (11) gives a stringent limit on $k_\perp^2/Q^2$. This leads, for instance, to a better description of some observables like the $\langle\cos\phi_h\rangle$ and $\langle\cos 2\phi_h\rangle$ asymmetries (central and right panel of fig. 2) and introduces some interesting effects in the $\langle P_T^2\rangle$ behaviors [23].

REFERENCES

[1] Mulders P. J. and Tangerman R. D., *Nucl. Phys. B*, **461** (1996) 197.
[2] Bacchetta A. *et al.*, *JHEP*, **02** (2007) 093.
[3] Anselmino M. *et al.*, *Phys. Rev. D*, **83** (2011) 114019.
[4] Anselmino M. *et al.*, *Eur. Phys. J. A*, **39** (2009) 89.
[5] Diefenthaler M., *Proceedings of DIS2007*, in *Prog. High Energy Phys.*, Vol. **1** (SciWiPub) 2007.
[6] Alekseev M. *et al.*, *Phys. Lett. B*, **673** (2009) 127.
[7] Martin A., *Czech. J. Phys.*, **56** (2006) F33.
[8] Airapetian A. *et al.*, *Phys. Rev. Lett.*, **103** (2009) 152002.
[9] Boer D. and Mulders P. J., *Phys. Rev. D*, **57** (1998) 5780.
[10] Anselmino M. *et al.*, *Phys. Rev. D*, **71** (2005) 074006.
[11] Gluck M., Reya E. and Vogt A., *Eur. Phys. J. C*, **5** (1998) 461.
[12] de Florian D., Sassot R. and Stratmann M., *Phys. Rev. D*, **75** (2007) 114010.
[13] Anselmino M. *et al.*, *Phys. Rev. D*, **72** (2005) 094007.
[14] Anselmino M. *et al.*, *PoS*, **DIS2010** (2010) 216.
[15] Collins J. C., *Nucl. Phys. B*, **396** (1993) 161.
[16] Anselmino M. *et al.*, *Nucl. Phys. Proc. Suppl.*, **191** (2009) 98.
[17] Seidl R. *et al.*, *Phys. Rev. D*, **78** (2008) 032011.
[18] Gluck M., Reya E., Stratmann M. and Vogelsang W., *Phys. Rev. D*, **63** (2001) 094005.
[19] Barone V., Melis S. and Prokudin A., *Phys. Rev. D*, **81** (2010) 114026.
[20] Kafer W., *Proc. of Transversity 2008* (World Scientific) 2008, p. 169.
[21] Bressan A., *Proceedings of DIS2009*, in *Prog. High Energy Phys.*, Vol. **3** (SciWiPub) 2009.
[22] Giordano F. and Lamb R., *AIP Conf. Proc.*, **1149** (2009) 423.
[23] Boglione M., Melis S. and Prokudin A., *Phys. Rev. D*, **84** (2011) 034033.